ICARUS 110, 196–202 (1994)

Assessment of Antipodal-Impact Terrains on Mars

DAVID A. WILLIAMS AND RONALD GREELEY

Department of Geology, Box 871404, Arizona State University, Tempe, Arizona 85287-1404
E-mail: williams@asuws2.la.asu.edu

Received November 4, 1993; revised May 23, 1994

The regions antipodal to Mars' three largest impact basins, Hellas, Isidis, and Argyre, were assessed for evidence of impact-induced disrupted terrains. Photogeology and computer modeling using the Simplified Arbitrary Lagrangian Eulerian (SALE) finite element code suggest that such terrains could have been formed by the Hellas impact. Maximum antipodal pressures are 1100 MPa for Hellas, 520 MPa for Isidis, and 150 MPa for Argyre. The results suggest that if antipodal fracturing were associated with later volcanism, then Alba Patera may be related to the Hellas event, as proposed by Peterson (*Lunar Planet. Sci.* 9, 885–886, 1978)). Alba Patera is a unique volcano in the solar system, being a shield volcano which emitted large volume lava flows. This volcanism could be the result of the focusing of seismic energy which created a fractured region that served as a volcanic conduit for the future release of large volumes of magma. No disrupted terrain features are observed antipodal to the Isidis or Argyre basins, although some of the old fractures in Noctis Labyrinthus could have originated in response to the Isidis impact, and later been reactivated by the Tharsis tectonics assumed to have produced Noctis. If the lower calculated antipodal pressures for Argyre were capable of producing disrupted terrains, then the terrains have been covered subsequently by volcanic or aeolian material, or modified beyond recognition.

INTRODUCTION

In the early 1970s anomalous terrains were discovered in regions antipodal to the Imbrium impact basin on the Moon (Wilhelms and McCauley 1971) and the Caloris impact basin on Mercury (Murray *et al.* 1974). Schultz (1972) and Schultz and Gault (1975) suggested that such terrains were produced by crustal disruption from the focusing of impact-generated seismic waves. Preliminary assessments for the Moon (Schultz and Gault 1975) and for Mercury (Hughes *et al.* 1977) suggested that the energy of a large impact could disrupt the antipodal surface. Although Mars has been studied in great detail, the question of antipodal-impact effects on Mars has been addressed only once (Peterson 1978). In this report we discuss applications of an antipodal-impact terrain model of Watts *et al.* (1991) to determine if impact-induced features could have occurred on Mars and outline results from photogeologic analysis of the antipodal-impact zones of Mars' three largest impact basins (Hellas, Isidis, and Argyre).

BACKGROUND

Wilhelms and McCauley (1971) first identified a "hilly and furrowed terrain," which is approximately antipodal to the Imbrium impact basin on the Moon, covering ~900 km^2 near Mare Ingenii. They suggested that the terrain (consisting of closely spaced, convex-up ridges and straight furrows) might have been produced by volcanic modification of basin ejecta. Murray *et al.* (1974) described a "weird terrain" (area of 900 km by 400 km) antipodal to the Caloris basin on Mercury that is morphologically similar to the lunar antipodal terrain.

Schultz (1972) and Schultz and Gault (1975) suggested that the antipodal formations on the Moon were produced by impact-induced seismic activity. They assessed this possibility, and found that the seismic energy of an Imbrium-size impact (600 km excavation cavity) could cause ground movement at the antipode of >10 m. Hughes *et al.* (1977) used a sophisticated finite element code to calculate large impact effects on a planet with either a solid or molten interior. They also discovered that ground displacement could occur at the antipode but, more importantly, noted that the calculated effects were stronger in a planet with a molten interior than in a solid planet. They attributed this result to the greater efficiency of energy-dissipation in solid material.

Watts *et al.* (1991) extended the work of Schultz and Gault (1975) to model impact effects on a two-layered planetary interior (mantle and core) and measure the influence of composition (silicate, iron, or water ice) on seismic wave propagation. They applied the results to the Moon, Mercury, and icy satellites. The calculations are based on a modified SALE (Simplified Arbitrary Lagrangian Eulerian) finite element code (Amsden *et al.* 1980) which predicts energy distributions from impacts, using a 2-dimensional half-circular computational grid. The pro-

0019-1035/94 $6.00

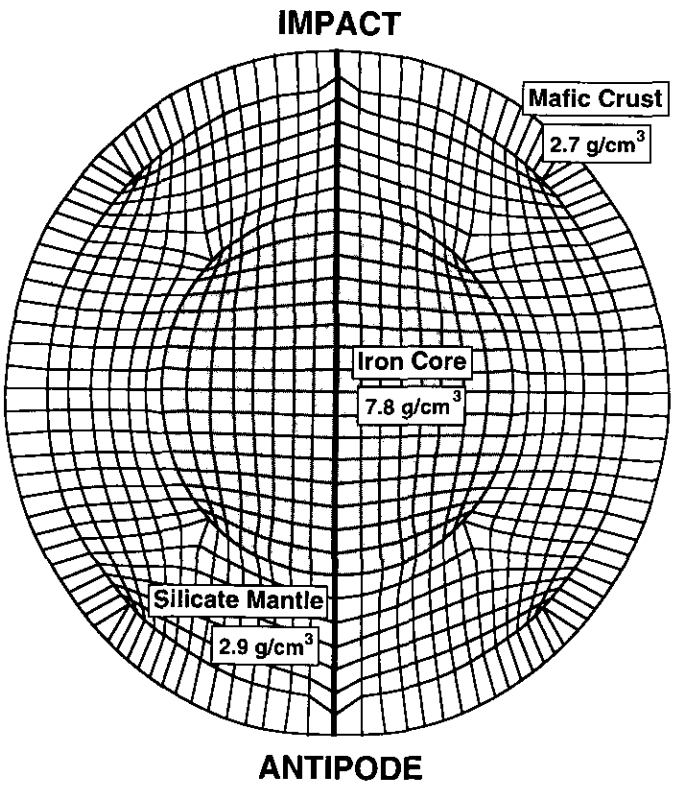

FIG. 1. SALE grid simulation of Mars. Reflective axis used to simulate full planet.

gram is initiated with parameters that specify the size and type of impact, the size and composition of the target planet, and the resolution of the computational net. The SALE program was adapted to simulate Mars for this study.

SALE IMPACT MODELING FOR MARS

Watts *et al.* (1991) describe in detail the configuration, initiation, and execution of the SALE program. Briefly, the energy required to simulate a specific Martian basin-forming impact is inserted into the model in the form of a high temperature, high density cell at the surface. The release of energy from this cell creates a spherical shock wave which propagates through the planet, simulated by the half-circular mesh, and may be focused at the antipode, producing antipodal features (Fig. 1). The first step in each experimental run is to set up the initial parameters, including the size and type of impact, the size and composition of the target planet, and the resolution of the computational net. The impact is modeled from the time just after the projectile strikes the surface.

An upper limit on the impact energy required to form a given size crater is derived from the Schmidt–Holsapple crater scaling equation (Melosh, 1989),

$$E_{SH} = \left[\frac{D_t}{1.8\rho_t^{-.33} g^{-.22}} \frac{1}{\rho_p^{.11} L_p^{.13}}\right]^{4.54}, \quad (1)$$

in which E_{SH} = total impact energy, D_t = transient crater diameter = $0.84D$ (rim-to-rim diameter), ρ_p = projectile density, ρ_t = Mars' surface density, g = Mars' gravity, and L_p = projectile diameter. Note that this equation assumes vertical impacts. Energy is inserted into the model in the form of a high temperature, high density cell. The density and internal energy of the target material, which has been appropriately compressed by the shock front, are calculated by the Rankine–Hugoniot equations of state and the pressure is calculated within SALE with the Tillotson equation of state (Tillotson 1962), which describe how shock pulses move through and affect solid material. This experimentally derived equation is used in two forms: (1) the material is compressed ($\rho/\rho_0 \leq 1$, internal energy $E < E_{iv}$, energy of incipient vaporization), and (2) the material is vaporized ($E > E_{iv}$). The compressed state equation is

$$P_* = \left[a + \frac{b}{E_i/E_0\eta^2 + 1}\right]\rho E_i + A\mu + B\mu^2, \quad (2)$$

and the expanded state equation is

$$P_* = a\rho E_i + \left[\frac{b\rho E_i}{E_i/E_0\eta^2 + 1} + A\mu e^{-\beta\zeta}\right] e^{-\alpha(\zeta)^2}, \quad (3)$$

in which ρ_0 = initial density, P_* = compressed or expanded pressure, ρ = current density, E_i = specific internal energy, $\eta = \rho/\rho_o$, $\zeta = \rho_o/\rho - 1$, $\mu = \eta - 1$, E_o = initial energy term, and α, β, a, b, A, and B are experimental parameters dependent on target material. A material fracture condition has been added to the equation of state, because pressures at the impact site exceed the vaporization pressure of the surface material, and the pressure and temperature at the wavefront will exceed the melting temperature after the shock front has passed. If the density in a cell has decreased to <90% of the initial density, the material is considered fractured and the pressure is set to zero. This correction is applied only within the crater itself and has very little effect outside the area of disruption. The purpose of this correction is to eliminate unreasonably high negative pressures in cells around the impact, which are composed mostly of fractured material (Watts *et al.* 1991). Where vaporized material moves away from the impact site at high velocity, the density, velocity, and pressure are set to zero in cells neighboring the impact site when they exceed the expansion criterion, which effectively removes them from the calculation. This correction eliminates the problem of overexpanded cells or

crossed vertices at the impact site when the grid moves with the material in the Lagrangian mode (Watts *et al.* 1991).

The SALE computational mesh is 30 cells long and 15 cells wide. A scale factor is applied to each cell to adapt the mesh for simulating Mars with a diameter of 6800 km (actual diameter 6796 km). We assume Mars was at its present diameter at the time of large basin formation 3.5–4.0 byr ago. The choice of interior model is limited to substances for which Tillotson equation of state parameters are available, and assumes a differentiated, nonmolten interior. The composition of the core of Mars is thought to be just on the iron side of the Fe–FeS eutectic, with a density of ~5000–7000 kg/m^3 (Johnston and Toksoz 1977). The radius of Mars's core is estimated to be between 1500 and 2000 km at present (Johnston and Toksoz 1977). For simplicity, we assumed that core size has not changed appreciably since the time of basin impacts, and an intermediate value of 1800 km was chosen. The mantle of Mars is thought to be enriched in FeO with an olivine composition of 75% forsterite with a density of 3550 kg/m^3 (Reasenburg 1977). The ancient crust of Mars is thought to be mafic (Carr 1981). The substances for which Tillotson values are available that most closely resemble these materials are andesite (for the crust, ρ = 2700 kg/m^3), low pressure phase anorthosite (for the mantle, ρ = 2900 kg/m^3), and solid iron (for the core, ρ = 7800 kg/m^3). We recognize that these values differ from those theorized for the Martian interior, but have chosen them because they are the best available which are associated with the calculated Tillotson parameters for each material. The effect of having a mantle too low in density and a core too high in density roughly balance in the model. In addition, recent work by Schubert and Spohn (1990) assumes that Mars was initially hot and completely differentiated into a mantle and core, with simple cooling and interior temperature and heat flux decreasing monotonically with time. If we acknowledge the results from Hughes *et al.* (1977) on the disruption produced from solid vs molten interiors, then our model functions as a lower limit on antipodal pressures produced by these three similar-aged Martian basins (Hellas, Isidis, and Argyre).

Because the outside boundary is a free surface, antipodal surface pressure equals zero and therefore the maximum pressures calculated by SALE are maximum values in the center of the antipodal cell, at a depth of 1/60 of the planetary diameter (Watts *et al.* 1991).

SOURCES OF UNCERTAINTY

Watts *et al.* (1991) detail the sources of uncertainty present in this technique. Briefly, uncertainties in the model come from two sources: inaccuracies that may be present in the Schmidt–Holsapple scaling equation and limitations imposed in the SALE code. The Schmidt–Holsapple equation has several limitations. Melosh (1989) compared the Gault scaling equation, the Schmidt–Holsapple equation, and the scaling equation of Nordyke (1962). He found good agreement between the three laws when calculating crater size from impact energy, but found that a factor of 40 uncertainty is introduced when calculating impact energy from crater size. Following the Watts *et al.* (1991) study, the Schmidt–Holsapple equation is used for these calculations, although the uncertainty remains high because the equation applies to the transient cavity, which is difficult to estimate on planetary surfaces (Watts *et al.* 1991). The kinetic energy of each impact is used as an additional constraint for determining impact energy (Schultz, personal communication).

The initial energy for a given impact is a function of impactor density ρ_p and diameter L_p. Calculations for a given impact basin size (transient crater diameter D_t derived from rim-massif boundary D using $D_t = 0.84D$, Melosh 1989, p. 129) with a range of impactors (Table I) yield impact energies which results in a 20% variation in antipodal pressure (Watts *et al.* 1991). Here we assume values for impactor size and diameter which are estimates derived from Schultz and Wichman (1990), Schubert and Matson (1982), and Schultz (personal communication): impact velocities ~5.2–15 km/sec, ρ_p = 2700–3300 kg/m^3, and L_p = 75–500 km. This uncertainty in the initial energy calculation, along with the inherent error in using scaling laws which cannot be validated experimentally, is the greatest source of error in this procedure.

It should be noted that calculations are slightly sensitive to grid configuration and timestep selection. However, these factors affect only the absolute values obtained, not the relative values for comparing one impact with another (Watts *et al.* 1991). The values cited for antipodal pressures generated by known impacts may be consistently too high or too low, but the relative pressure differences for different-sized impacts modeled on the same planet are unaffected.

RESULTS

The program was run for each impact that formed one of the Martian basins. E_{SH} is calculated for each basin, and that energy is input into the half-circular grid simulating Mars. The energy is attenuated through the interior from impact to antipode, and pressures in the antipodal cells are recorded. The values of maximum antipodal pressure for Martian impacts can then be compared to those determined for the Imbrium impact on the Moon and the Caloris impact on Mercury with their appropriate internal structures (Watts *et al.* 1991) using the same approach (Table II).

The Schultz and Gault (1975) calculations were made

TABLE I
Variation in Impact Energy and Antipodal Pressure Resulting from a Range of Impactor Parameters in SALE Modeling Results for Martian Impacts

D_t (m)	ρ_p (kg/m^3)	L_p (m)	E_{SH} (J)	v (m/s)	E_{imp} (J)	Variation in Antipodal Pressure (Pa)
Hellas						
1.512E6	2700	3.0E5	4.5E27	15,000	4.3E27	6.6E8-1.5E9
1.512E6	2900	5.0E5	3.2E27	6,000	3.4E27	9.9E8-1.2E9
1.512E6	3300	3.8E5	3.5E27	9,000	3.8E27	8.8E8-1.3E9
Isidis						
1.008E6	2900	2.5E5	7.6E26	8,000	7.6E26	3.1E8-7.3E8
1.008E6	3300	1.8E5	8.7E26	13,000	8.5E26	2.1E8-8.3E8
1.008E6	3300	3.0E5	6.4E26	5,200	6.3E26	4.4E8-6.0E8
Argyre						
5.04E5	3300	7.5E4	6.3E25	13,000	6.2E25	6.0E7-2.4E8
5.04E5	3300	1.0E5	5.3E25	8,000	5.5E25	9.0E7-2.1E8

Note. Target density for all calculations is 2700 kg/m^3, Mars gravity is 3.7 m/s^2, v is impact velocity, E_{imp} is kinetic energy of impact.

assuming a lunar density of 3300 kg/m^3 and an upper lunar crust density of 3000 kg/m^3. They found that the tensile stress resulting from the reflection of a compressive wave into a tensile wave at the basin antipode exceeded the tensile strength of most common rocks, and could cause fracture and spallation. A saw-toothed tensile wave emerging from a solid body will spall the body with a thickness $(\sigma_\chi/\sigma)(\lambda/2)$ and velocity $(2\sigma - \sigma_\chi)/\rho c$, where σ_c is the tensile strength of the material, σ is the normal stress, λ is the wavelength of the wave, ρ is body density, and c is wave velocity (Rinehart 1960). Hence an Imbrium-sized impact on a homogeneous Moon would create an antipodal spall of thickness 110 km and velocity of 1.5 m/sec. While the tensile strength will probably be

TABLE II
SALE Modeling Results for Martian Impacts

Planet	Diameter (km)	Basin	Diameter (km)	I/P*	E_{SH} (J)	Antipodal Pressure (Pa)
Mercury	4878	Caloris	1092	0.224	2.0E31	5.7E9^
Moon	3600	Imbrium	600	0.140	6.1E27	1.9E9^
Mars	6794	Hellas	1512	0.224	2.7E27	1.1E9
Mars	6796	Isidis	1008	0.148	5.7E26	5.2E8
Mars	6796	Argyre	504	0.074	3.3E25	1.5E8

* Impact to planet ratio.
^ From Watts *et al.* (1991).

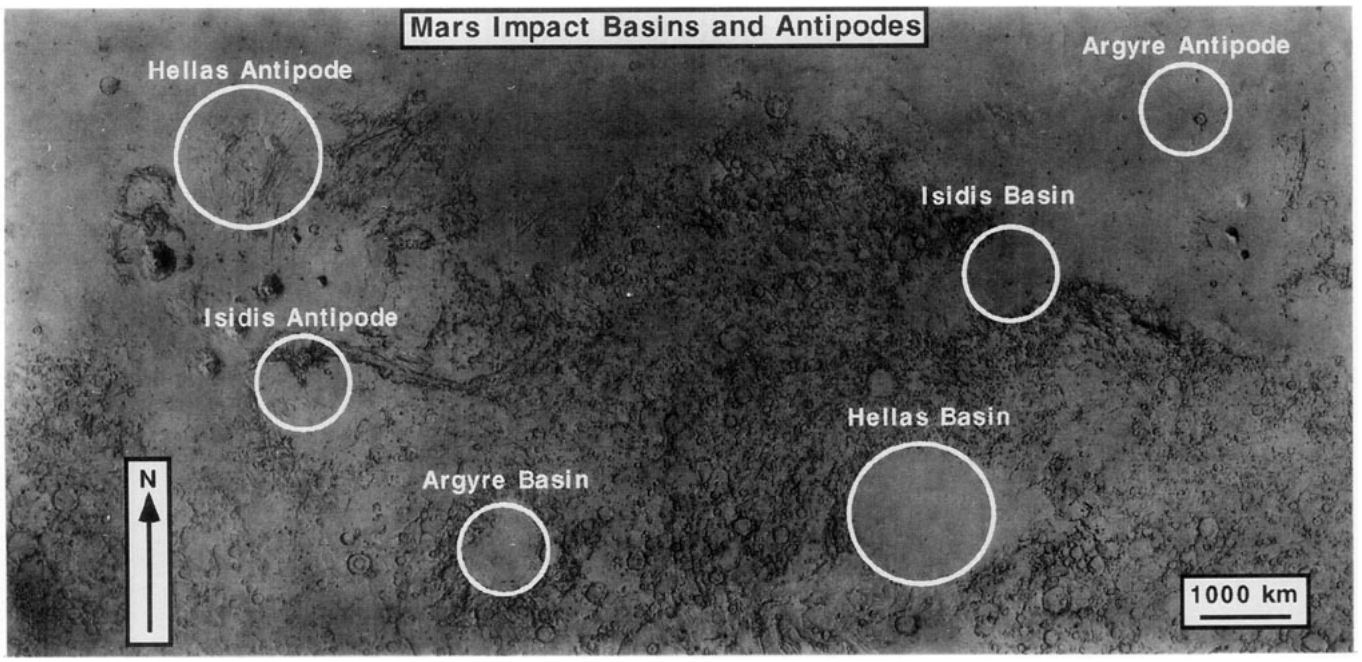

FIG. 2. Mars's major impact basins and their antipodes.

increased at such depths due to gravity loading and may prevent spallation, the crustal fractures and preexisting joints should encourage failure (Schultz and Gault 1975).

We find that the values of maximum antipodal pressure calculated for the Hellas impact are similar to those values calculated for the Caloris impact on Mercury and the Imbrium impact on the Moon. This result suggests that disrupted antipodal terrains could have been produced by this impact. However, calculated antipodal pressures for the Isidis and Argyre impacts are lower, and antipodal terrain may not have been generated.

PHOTOGEOLOGY OF ANTIPODAL ZONES

In order to assess the potential effects of large impacts on Mars, a photogeological search using Viking Orbiter photographs was conducted for the theorized disrupted terrains in zones antipodal to the Hellas, Isidis, and Argyre basins (Fig. 2). Based on the sizes of the regions covered by antipodal terrains on the Moon and Mercury, the size of the search zone was arbitrarily set equal to the diameter of the given Martian basin, centered on the antipodal point of the basin. If seismic waves are focused on the antipode from an impact, disruption should occur in this zone, assuming spherical symmetry of the interior layers.

The center of the Hellas basin lies at 40°S, 292°W (Peterson 1977); antipodal to this, at 40°N, 112°W, is the caldera of the volcano Alba Patera. Alba Patera is a central-vent volcano more than 1500 km across with flank slopes <0.1° (Greeley and Spudis 1981). The Hellas antipodal zone includes lava flows from Alba Patera of Amazonian and Hesperian ages (Scott and Tanaka 1986). If we assume that the Martian basin impacts occurred in the waning stages of the heavy bombardment thought to have taken place in the early solar system (early to mid Noachian age on Mars), then any antipodal terrain like that observed on the Moon or Mercury would be covered by post-impact materials, such as the younger lava flows of Alba. Hence, other possible indicators of antipodal activity on Mars must be assessed, as was done by Peterson (1978). For example, he suggested that focusing of seismic shocks from the Hellas impact might have produced the volcanic conduit at Alba Patera through which magma could reach the surface.

Wood and Head (1976) place the center of the Isidis basin at 16°N, 272°W for a crater diameter of 1900 km; Peterson (1978) gives the center at 15°N, 271°W. The corresponding antipode would be at 15°S, 91°W in Sinai Planum ~400 km SSE of the "center" of Noctis Labyrinthus. The Isidis antipodal zone includes most of Noctis Labyrinthus and Tithonium Chasma, and part of Ius Chasma. This zone is characterized by Hesperian volcanic features, a tectonically fractured unit, and deposits on the walls and floors of canyons. There are no Noachian-age deposits in the zone. However, Peterson (1977) suggested that older fractures in Noctis Labyrinthus may have been generated or modified by the Isidis impact.

The center of the Argyre basin is ~51°S, 42°W. Antipo-

dal to this, at 51°N, 222°W, is a point in Utopia Planitia, ~250 km NE of the Viking Lander 2 site. Rocks in the zone consists of Hesperian-age deposits of volcanic, alluvial, and/or aeolian origin. Small, dark, knob-like hills with some summit craters are also present. No Noachian-age material or unusual features occur in the zone.

DISCUSSION

Our results suggests that antipodal pressures from the Hellas impact probably produced sufficient focused energy at its antipode to produce deep fractures (on the order of tens of kilometers) in the Martian crust centered below the current caldera for Alba Patera, and may account for aspects of volcanism at Alba. Alba Patera has long been recognized as unusual (Carr *et al.* 1977). It is a "central-vent" volcano containing a caldera complex ~100 km across and has flows that can be traced more than 1000 km, making it the largest such volcano in the solar system. Studies of the Alba flows (Greeley and Spudis 1981, Cattermole 1987, 1990) indicate high rates of effusion and an early-Hesperian phase of flood-type volcanism, perhaps similar to continental flood volcanism as in the Columbia River Basalt Province, followed by later eruption of high-volume sheet and tube-fed lavas from fissures. Certain long flows seen on the Moon are inferred to have been derived from fissures associated with basin-related fractures (Schaber 1973). Moreover, the low flank slopes of Alba Patera may indicate a different style of volcanism from that of the other Tharsis volcanoes on Mars, all of which are high-standing edifices. Perhaps a Hellas-produced antipodal fracture system could have provided a ready conduit for early-stage eruptions of Martian lavas derived from deep in the crust/upper mantle in the Tharsis area. These fluid lavas would have erupted at high rates from the central zone of the antipodal fractures and spread to great distance to form the basal lavas of Alba Patera. This occurred in the Hesperian, $\sim 1.5 \times 10^9$ years after Hellas disrupted the antipodal interior. The change in morphology to tube-fed flows at Alba Patera for the later deposits suggests lower rates of effusion of a sporadic character (Greeley and Spudis 1981), which may reflect lower rates of magma production, more constrained conduits, more "evolved" magmas, or some combination of these factors. Although the Hellas basin itself is apparently not flooded by lavas, as are Imbrium and Orientale on the Moon, there is evidence of antipodal volcanism on the Moon (Mare Ingenii opposite Imbrium, Mare Marginis opposite Orientale). This lunar antipodal volcanism occurs in basins themselves, in which the far-side crust has been excavated by the Ingenii and Marginis events, respectively. These events additionally would facilitate the emplacement of mare lava flows.

The computer model gives antipodal pressures for the Isidis impact approximately half those calculated for the Imbrium impact, suggesting that disrupted terrains may not have been produced. No such terrains are observed, although Peterson (1978) suggested that some of the fractures of the Noctis Labyrinthus system may have been generated or influenced by the Isidis impact. Some of the fractures in the Noctis Labyrinthus system are radial to or concentric about the Isidis antipode. Carr (1974) suggested that this topographically high region might be due to crustal upwarping caused by mantle convection in Tharsis. The load from Tharsis volcanics may have reactivated certain aligned older fractures, previously emplaced by Isidis antipodal activity (Peterson 1978). Thus, Noctis Labyrinthus may be a younger feature that owes its location at least partly to the antipodal effects of a major impact. However, such reactivation of preexisting fractures has not been observed at lunar basin antipodes. The lack of visible features at the Argyre antipode suggests that either the low antipodal pressures were insufficient to disrupt the terrain, or such terrain was produced but has since been obliterated.

ACKNOWLEDGMENTS

The authors thank Bob Altum and Larry Bolef for help with the computer simulations, David Crown and Byron Schneid for stimulating conversations on this research, and James Tyburczy, Christopher Sanders, David R. Williams, Peter Schultz, and Daniel Janes for review comments and suggestions. The authors especially acknowledge the assistance of Alison Watts, whose discussions enabled us to modify the SALE program for this project. This work was supported by the Office of Planetary Geology, National Aeronautics and Space Administration.

REFERENCES

AMSDEN, A. A., H. M. RUPPEL, AND C. W. HIRT 1980. *SALE: A Simplified ALE Computer Program for Fluid Flow at All Speeds.* Report LA-8095, Los Alamos Scientific Laboratory, New Mexico.

CARR, M. H. 1981. *The Surface of Mars.* Yale Univ. Press, New Haven, CT.

CARR, M. H., K. R. BLASIUS, R. GREELEY, J. E. GUEST, AND H. MASURSKY 1977. Observations on some martian volcanic features as viewed from the Viking orbiters. *J. Geophys. Res.* **82,** 3985–4015.

CARR, M. H. 1974. Tectonism and volcanism of the Tharsis region of Mars. *J. Geophys. Res.* **79,** 3943–3949.

CATTERMOLE, P. 1987. Sequence, rheological properties, and effusion rates of volcanic flows at Alba Patera, Mars. In *Proceedings, 17th Lunar Planetary Science Conference,* pp. E553–E560.

CATTERMOLE, P. 1990. Volcanic flow development at Alba Patera, Mars. *Icarus* **83,** 453–493.

GREELEY, R., AND P. D. SPUDIS 1981. Volcanism on Mars. *Rev. Geophys. Space Phys.* **19,** 13–41.

HUGHES, H. G., F. N. APP, AND T. R. MCGETCHIN 1977. Global seismic effects of basin forming impacts. *Phys. Earth Planet. Interiors* **15,** 251–263.

JOHNSON, D. H., AND M. N. TOKSOZ 1977. Internal structure and properties of Mars. *Icarus* **32,** 73–84.

MELOSH, H. J. 1989. *Impact Cratering: A Geologic Process*. Oxford Univ. Press, New York.

MURRAY, B. C., M. J. BELTON, G. E. DANIELSON, M. E. DAVIES, D. E. GAULT, B. HAPKE, B. O'LEARY, R. G. STROM, V. SUOMI, AND N. TRASK 1974. Mercury's surface: Preliminary description and interpretation from Mariner 10 pictures. *Science* **185,** 169–179.

NORDYKE, M. D. 1962. An analysis of cratering data from desert alluvium. *J. Geophys. Res.* **67,** 1965–1974.

PETERSON, J. E. 1978. Antipodal effects of major basin-forming impacts on Mars, (abstract). *Lunar Planet. Sci.* **9,** 885–886.

PETERSON, J. E. 1977. *Geologic Map of the Noachis Quadrangle of Mars, Scale 1:5,000,000*. Misc. Inv. Series Map I-910, U.S. Geol. Surv., Reston, VA.

REASENBERG, R. D. 1977. The moment of inertia and isostacy of Mars. *J. Geophys. Res.* **82,** 369–375.

RINEHART, J. S. 1960. *Q. Colo. Sch. Mines* **55**.

SCHABER, G. G. 1973. Lava flows in Mare Imbrium: Geologic evaluation from Apollo orbital photographs. In *Proceedings, 4th Lunar Science Conference*, pp. 73–92.

SCHUBART, J., AND D. L. MATSON 1982. Masses and densities of asteroids. In *Asteroids* (T. Gehrels, Ed.), pp. 84–97. Univ. of Arizona Press, Tucson.

SCHUBERT, G., AND T. SPOHN 1990. Thermal history of Mars and the sulfur content of its core. *J. Geophys. Res.* **95,** 14,095–14,104.

SCHULTZ, P. H. 1972. *A Preliminary Morphologic Study of the Lunar Surface*. Ph.D. thesis, Univ. of Texas at Austin, Austin, Texas.

SCHULTZ, P. H. 1976. *Moon Morphology*. Univ. of Texas Press, Austin, Texas.

SCHULTZ, P. H., AND D. E. GAULT 1975. Seismic effects from major basin formation on the Moon and Mercury. *The Moon* **12,** 159–177.

SCHULTZ, P. H., AND R. W. WICHMAN 1990. Contamination of the Martian mantle by basin-forming impactors (abstract). In *MEVTV Workshop on the Evolution of Magma Bodies on Mars*, pp. 37–38.

SCOTT, D. H., AND K. L. TANAKA 1986. *Geologic Map of the Western Equatorial Region of Mars, Scale 1:15,000,000*. Misc. Inv. Series Map I-1802-A, U.S. Geol. Surv., Reston, VA.

SCOTT, D. H., AND M. H. CARR 1978. *Geologic Map of Mars, Scale 1:25,000,000*. Misc. Inv. Map I-1083, U.S. Geol. Surv., Reston, VA.

TILLOTSON, J. H. 1962. *Metallic Equations of State for Hypervelocity Impacts*. General Atomic Report GA-3216, John Jay Hopkins Lab. for Pure and Applied Science, San Diego.

WATTS, A. W., R. GREELEY, AND H. J. MELOSH 1991. The formation of terrains antipodal to major impacts. *Icarus* **93,** 159–168.

WILHELMS, D. E., AND J. F. MCCAULEY 1971. *Geologic Map of the Near Side of the Moon, Scale 1:5,000,000*. Geol. Inves. Map I-703, U.S. Geol. Surv., Reston, VA.

WOOD, C. A., AND J. W. HEAD 1976. Comparisons of impact basins on Mercury, Mars, and the Moon. In *Proceedings, 7th Lunar Science Conference*, pp. 3629–3651.